ACS APPLIED MATERIALS & INTERFACES

Research Article

www.acsami.org

In situ Synthesis of Polymer-Modified Mesoporous Carbon CMK-3 Composites for CO_2 Sequestration

Chih-Chau Hwang,[†] Zhong Jin,[†] Wei Lu,[†] Zhengzong Sun,[†] Lawrence B. Alemany,[†,‡] Jay R. Lomeda,[§] and James M. Tour*[,†,‡,⊥]

[†]Department of Chemistry and [‡]The Smalley Institute for Nanoscale Science and Technology, Rice University, Houston, Texas 77251, United States

[§]Nalco Energy Services Headquarters, 7705 Highway 90-A, Sugar Land, Texas 77478, United States

[⊥]Department of Mechanical Engineering and Materials Science, Rice University, MS-222, 6100 Main Street, Houston, Texas 77005, United States

Supporting Information

ABSTRACT: Here we report carbon-based composites polyethylenimine-mesocarbon (PEI-CMK-3) and polyvinylamine-mesocarbon (PVA-CMK-3) that can be used to capture and rapidly release CO_2. CO_2 uptake by the synthesized composites was determined using a gravimetric method at 30 °C and 1 atm; the 39% PEI-CMK-3 composite had ∼12 wt % CO_2 uptake capacity and the 37% PVA-CMK-3 composite had ∼13 wt % CO_2 uptake capacity. A desorption temperature of 75 °C was sufficient for regeneration. The CO_2 uptake was the same when using 10% CO_2 in a 90% CH_4, C_2H_6, and C_3H_8 mixture, underscoring this composite's efficacy for CO_2 sequestration from natural gas.

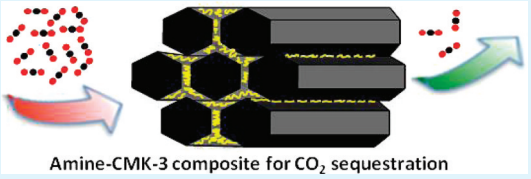

KEYWORDS: *CO_2 sequestration, mesoporous carbon (CMK-3), in situ polymerization, solid-supported amine sorbents, impregnation, polymer-carbon composites*

INTRODUCTION

Since the industrial revolution, CO_2 emissions from fuel combustion have been growing rapidly. The increased CO_2 concentration in the atmosphere might contribute to apparent global warming and serious climate change. Reducing CO_2 emissions from industrial and natural gas streams therefore becomes an important issue. Furthermore, sequestration of CO_2 from atmospheric pressure environments is important in life-support systems in space and under water where compression is discouraged due to the energy penalty.[1] Recently, CO_2 capture and sequestration have been receiving significant attention. Several chemical and physical methods were developed for CO_2 separation at near-atmospheric pressure. For instance, liquid sorbents made by aqueous amine species have been developed for commercial CO_2 separation.[2,3] Even though aqueous amines have low cost and high efficacy, their regeneration requires high energy input. In keeping with the worldwide trend toward safer and cleaner processes, more environmentally friendly and less energy intensive solid sorbents are being developed to replace the conventional liquid sorbents. Activated carbon, one of the most common solid sorbents, is an extremely porous material that has been widely used as an industrial sorbent because of its high surface area and relatively high CO_2 capacity.[3,4] Unfortunately, activated carbon has poorly controlled pore size distribution as well as a small pore volume, limiting its usefulness in CO_2 sorption. The grafting of amine functionalities onto a well-ordered solid support with a high surface area would combine the attractive features of the liquid sorbents with those of the solid sorbents. Accordingly, many types of amine-functionalized porous materials, such as M41S mesoporous silicas,[5−7] have been used for CO_2 sequestration due to their high surface area and tunable pore sizes. Scaroni et al. invented "molecular basket" CO_2 adsorbents based on the solid sorbent MCM-41 modified with polyethylenimine; this material had a ∼3.0 mmol/g (∼11.7 wt %) CO_2 capacity at 75 °C.[7] Because the amine species were physisorbed on the support through impregnation rather than covalent modification, there is concern regarding the materials' long-term stability over many reuse cycles since desorption of the amine functionalization might occur. Metal oxide frameworks (MOFs) are a class of sequestration materials that can reach 26% CO_2 uptake by weight at 25 °C and 1 atm,[8−11] but their ability to sequester CO_2 in the presence of small hydrocarbons might be limited because of their poorer selectivity.

Over the last few decades, there have been significant advances in the synthesis of mesoporous carbon materials, such as CMK-3 and CMK-5.[12−14] Ryoo et al. proposed a practical method through in situ polymerization to synthesize polymer-CMK-3 composites.[15] The mesocarbon CMK-3 is different from conventional carbon materials such as activated carbon due to its highly ordered meso-structure and high surface area.

Received: September 19, 2011
Accepted: November 17, 2011
Published: November 17, 2011

Downloaded via NORTHWEST UNIV on July 14, 2019 at 23:29:43 (UTC).
See https://pubs.acs.org/sharingguidelines for options on how to legitimately share published articles.

 © 2011 American Chemical Society

Scheme 1. Synthesis Processes to Produce Mesoporous Polymer−Carbon Composites PEI-CMK-3 and PVA-CMK-3

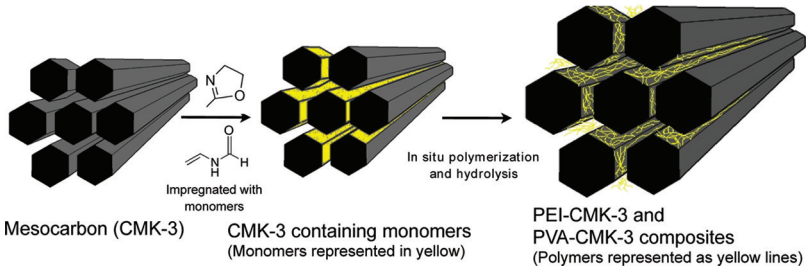

This allowed for the chemical properties of these composites to be maintained while greatly enhancing their thermal stability. Inspired by their work, we developed a route to synthesize polymer-mesocarbon composites that would lead to higher degrees of CO_2 sorption by the in situ polymerization of amine species to produce polyethylenimine (PEI) and polyvinylamine (PVA) inside the mesocarbon CMK-3. In addition to a high efficiency for CO_2 capture, they should also exhibit high stability due to the formation of interpenetrating composite frameworks between the entrapped polymers and mesocarbon CMK-3. Moreover, their uptake of small hydrocarbons should be minimal, making them suitable for use in CO_2 sequestration from natural gas streams.

RESULTS AND DISCUSSION

Here, mesoporous silica SBA-15 synthesized by the surfactant-assisted method[16] was used as a hard template to prepare mesoporous carbon CMK-3 as in the previous report.[17] Scheme 1 demonstrates the synthesis route to the desired polymer-mesocarbon composites PEI-CMK-3 and PVA-CMK-3. For the synthesis of the PEI-CMK-3 composite, the as-synthesized CMK-3 was suspended in a solution containing 2-methyl-2-oxazoline monomers and acetonitrile. The monomers started filling the mesopores by capillary condensation, and the wall surface of the CMK-3 was coated with a thin film of monomers after evaporation of the acetonitrile at 80 °C. $BF_3{\cdot}Et_2O$ was used as a catalyst and was subsequently added for the polymerization step. A similar methodology was carried out for the PVA-CMK-3 synthesis except *N*-vinylformamide and 2,2′-azobis(2-methylpropionitrile) (AIBN) were used as the monomer and catalyst, respectively. The polymer-CMK-3 composites needed to be further hydrolyzed, thus becoming the PEI-CMK-3 and PVA-CMK-3 composites. More details are described in the experimental section.

Attenuated total reflectance infrared (ATR-IR) analysis and ^{13}C NMR analysis were chosen to monitor the resultant composites during the synthetic processes. Figure 1a is the IR spectrum from CMK-3 impregnated with 2-methyl-2-oxazoline. The spectrum has a characteristic absorption band at 1673 cm^{-1} that can be assigned to a symmetric stretching mode of C═N from the 2-methyl-2-oxazoline. The presence of the *N*-substituted polyaziridine, generated from the ring-opening of 2-methyl-2-oxazoline, can be evidenced by a development of the characteristic C═O stretching at 1632 cm^{-1} as well as a disappearance of the original C═N vibration (Figure 1b). Figure 1c is a spectrum of the composite after hydrolysis with aqueous NaOH for 12 h; the characteristic peaks of the *N*-substituted polyaziridine from Figure 1b are replaced by peaks at 3260 and 1605 cm^{-1} that are assigned to N−H stretching and bending, respectively, from the secondary amine. In Figure 1d, a sharp peak together with a shoulder appear at 1636 and

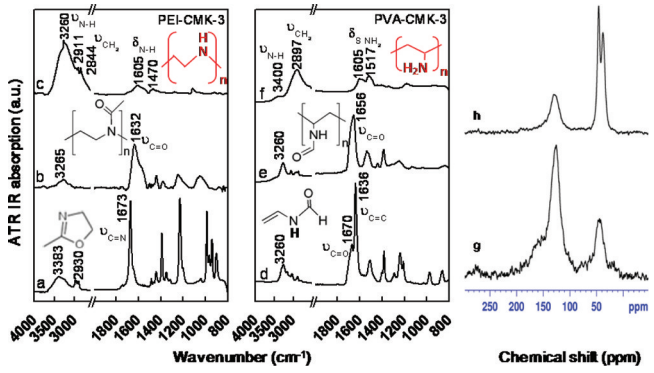

Figure 1. ATR-IR and solid-state $^1H-^{13}C$ CPMAS NMR spectra for (a−c, g) PEI-CMK-3 composite and (d−f, h) PVA-CMK-3 during the synthetic processes.

1670 cm^{-1}, corresponding to the C═C and C═O symmetric stretching from the *N*-vinylformamide monomers in CMK-3. Figure 1e shows a strong peak centered at 1656 cm^{-1} that is due to C═O stretching from the poly(*N*-vinylformamide) in the CMK-3 composite after the in situ polymerization. The structure of the PVA-CMK-3 composite was confirmed by the peaks around 3400 and 1605 cm^{-1} in Figure 1f because of the N−H stretching and NH_2 scissoring on the primary amine, respectively.

The molecular structures of PEI-CMK-3 and PVA-CMK-3 composites were further investigated by solid-state NMR analysis. ^{13}C MAS NMR spectra were acquired using $^1H-^{13}C$ cross-polarization (CPMAS) with contact time of 1 ms. Figure 1g shows that the PEI-CMK-3 composite has two main signals observed at $\delta \sim 126$ ppm and $\delta \sim 45$ ppm corresponding to sp^2-carbons from CMK-3 itself and to the $-CH_2-$ units of linear PEI, respectively. A minor shoulder around 165 ppm assigned to the carbamate[18] is assumed to arise through the composite reaction with CO_2 from the atmosphere during its storage. For the PVA-CMK-3 composite, the three carbon atom resonance peaks shown in Fig. 1h were assigned as follows: a sp^2-carbon peak ($\delta \sim 130$ ppm) from CMK-3 itself, a strong ($\delta \sim 46$ ppm) and a medium resonance ($\delta \sim 38$ ppm) attributed to the methine- and methylene moieties of the PVA main chain.

Transmission electron microscopy (TEM) and scanning electron microscopy (SEM) analyses were conducted to determine the morphologies and microstructures of the synthesized polymer-CMK-3 composites. A TEM image of the 39% PEI-CMK-3 parallel to the pore direction is shown in the Figure 2a. The small angle X-ray diffraction pattern (inset) clearly reveals the presence of hexagonally ordered porous structures for the produced polymer-CMK-3 composites. These ordered porous structures

dx.doi.org/10.1021/am201278c | ACS Appl. Mater. Interfaces 2011, 3, 4782–4786

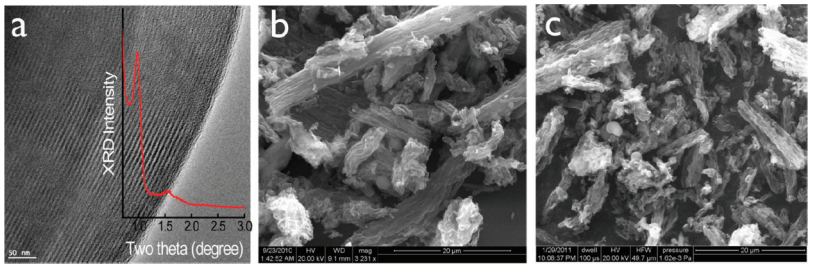

Figure 2. (a) TEM and (b) SEM images taken from the 39% PEI-CMK-3. The crystalline structure for the PEI-CMK-3 was observed by powder XRD (inset of a). (c) SEM image of the 37% PVA-CMK-3 composite. The scale bars for a–c are 50 nm, 20 μm, and 20 μm, respectively.

remain even after polymerization and hydrolysis. Images b and c in Figure 2 are SEM images taken of PEI-CMK-3 and PVA-CMK-3, respectively. Little bulk aggregation of polymer was observed on the outer surface, which means that the polymerization of PEI and PVA is primarily confined within the pores of the CMK-3. The resultant polymers form interpenetrating and inseparable composite frameworks with CMK-3, in good agreement with the high stability results obtained from the CO_2 sorption cycle study.

The porous nature of the polymer-CMK-3 composites was further characterized by nitrogen adsorption isotherms, which allow calculation of specific surface area, pore volume and pore size distribution (see Table 1). Pure CMK-3 has a high surface area of 1350 m^2/g with its pore volume of 1.40 cm^3/g and pore diameter of 3.9 nm. The actual loading of each polymer in the CMK-3 was determined by thermogravimetric analysis (TGA). The PEI-CMK-3 and PVA-CMK-3 behave similarly as their loadings were increased up to ~40 wt %. As the polymer loading of CMK-3 increased, the more meso- and micro-channels were occupied, leading to a corresponding decrease in the surface area and pore volume. As the polymer loading increased to over 50%, less than 1/10 original surface area and pore volume remained, causing mesopore blockage.

Table 1. Physical Properties of Selected Polymer Sorbents and Corresponding CO_2 Capacity

sorbents	surface area (m^2/g)	pore volume (cm^3/g)	pore size (nm)	CO_2 capacity (mmol/g)	CO_2 capacity (wt %)
CMK-3	1352	1.40	3.9	1.55	6.4
17% PEI-CMK-3	1248	1.26	3.4	2.00	8.1
28% PEI-CMK-3	950	0.66	3.2	2.36	9.4
39% PEI-CMK-3	774	0.49	2.9	3.13	12.1
52% PEI-CMK-3	134	0.19	0.5	0.49	2.1
21% PVA-CMK-3	1106	1.25	3.4	2.60	10.3
30% PVA-CMK-3	868	0.61	3.1	3.49	13.3
37% PVA-CMK-3	711	0.46	2.9	3.52	13.4
54% PVA-CMK-3	112	0.20	0.3	0.54	2.3
40%PEI-CMK-3 (impregnated)	315	0.27	0.6	1.95	7.9
40%PVA-CMK-3 (impregnated)	237	0.22	0.6	1.48	6.1

In addition to the monomer-infused composites, we also tried direct polymer impregnation to yield PEI-CMK-3 (impregnated) and PVA-CMK-3 (impregnated). These latter polymer-impregnated composites had lower surface areas and pore volumes than those made by the original in situ polymerization (Table 1), hence channel blockage results from this approach.

Thermogravimetric analysis (TGA) was applied to evaluate the potential sorption of CO_2 for the PEI-CMK-3 and PVA-CMK-3 composites. All of samples were pretreated at 100 °C under argon to remove moisture and other adsorbates. Once the chamber was cooled and temperature equilibrium (30 °C) was achieved, the gas flow in the TGA instrument was switched to CO_2 so as to pass through the sorbents. The CO_2 capacities of the sorbents with various amine species and loadings were measured at 30 °C and 1 atm and the results are summarized in Table 1. A capacity of 6.4 wt % (1.55 mmol/g) was obtained after feeding CO_2 to the pure CMK-3 over 30 min. In the case of PEI-CMK-3 composites, the sorption quickly reached a plateau with CO_2 uptake capacities between 8.1 and 12.1 wt % (3.13 mmol/g) as the PEI loading of the CMK-3 increased from 17 to 39 wt %. The capacities of the PVA-CMK-3 sorbents were improved from 10.3 to 13.4 wt % (3.52 mmol/g) with respect to similar PEI loadings. The ability of the PEI- and PVA-CMK-3 sorbents to capture CO_2 could be related to the number of amine groups for reaction and the 2° vs. 1° amine difference in the two. In addition, the CO_2 capacities for the PEI-CMK-3 (impregnated) and PVA-CMK-3 (impregnated) were almost 2-fold less than that of PEI-CMK-3 and PVA-CMK-3 sorbents made through the in situ polymerization method. The decreases in their CO_2 capacities were likely due to plugging of the pores by polymer chains. Because mesoporous carbon CMK-3 has a hydrophobic framework, hydrophilic polymers might not easily infiltrate into the mesoporous channels of CMK-3, resulting in polymer agglomeration outside the CMK-3. Higher loadings of polymers (such as 52% PEI-CMK-3 and 54% PVA-CMK-3) likely blocked the mesoporous channels, causing CO_2 diffusional limitations. These results are summarized in Table 1.

In addition to the high CO_2 capture efficiency, long-term stability and low-cost regeneration are also important concerns for any CO_2 sequestration system. In our case, as CO_2 was introduced into the sorbents, each CO_2 uptake cycle is a two-stage process, with the mass increasing significantly in the first stage in less than 5 min, followed by a second much slower sorption process until a stable maximum was reached (Figure 3). This two-stage sorption kinetics had been observed in other amine-impregnated sorbents.[19−21] Note that the capacity of the 37% PVA-CMK-3 is higher than 13 wt % within the first CO_2 exposure stage. The amine-based polymers are known to react with CO_2 to produce carbamates through the formation of zwitterionic intermediates. The rapid sequestration process is desirable for shortening the CO_2 sorption time. To check the stability of the composite sorbents, after the first sorption cycle, the cycling was repeated by heating the PEI-CMK-3 and

dx.doi.org/10.1021/am201278c | ACS Appl. Mater. Interfaces 2011, 3, 4782–4786

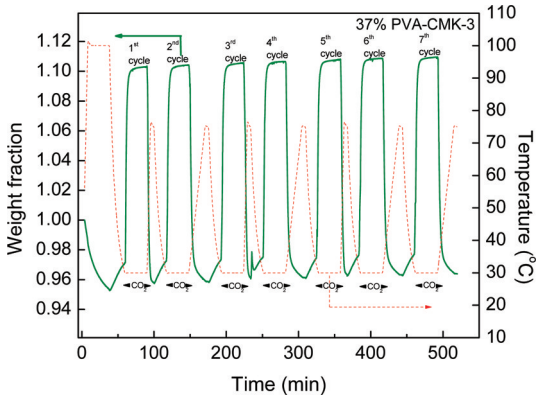

Figure 3. Sorption cycles of CO_2 studied by TGA at 30 °C on the 37% PVA-CMK-3 sorbent. The composite was first pretreated at 100 °C under argon to remove moisture and residual CO_2 followed by dosing with a 100% CO_2 gas stream (30 °C, 1 atm) for 30 min. After the first sorption cycle, the cycling was repeated by heating the adsorbent to 75 °C under argon for regeneration. The CO_2 uptake capacity was calculated based on the difference between the weight before and after CO_2 uptake using the raw data without further normalization.

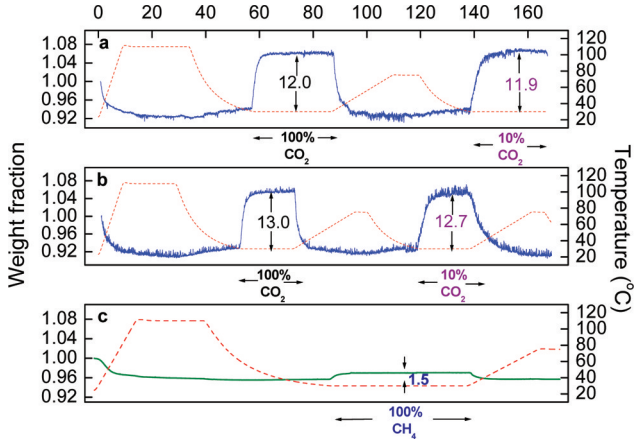

Figure 4. CO_2 uptake tests on (a) PEI-CMK-3 and (b) PVA-CMK-3 composites. The first uptake used pure CO_2, followed by the second uptake using 10% CO_2 flow (the balance was 85% CH_4, 3% C_2H_5 and 2% C_3H_8). (c) Pure methane adsorbed on the PVA-CMK-3 composite.

PVA-CMK-3 composites to 75 °C under argon gas for regeneration, followed by cooling to room temperature for another CO_2 capture. The 75 °C regeneration temperature is lower than that needed for silica-based amine sorbents, which is typically higher than 100 °C.

It has been known that the CO_2 sorption by "molecular baskets" is very sensitive to temperature.[7] The 37% PVA-CMK-3 sorbent was exposed to pure CO_2 at a temperature range from 30 to 75 °C. Clearly, as the temperature was increased, the composite reached a new sorption equilibrium. A plot of equilibrium CO_2 sorption versus temperature is given in Figure 1S. Furthermore, higher humidity improved the CO_2 capacity for amine-containing sorbents.[22] Therefore we compared the CO_2 uptake efficiency for the PVA-CMK-3 sorbent under dry and moist conditions at 30 °C (see Figure 2S in the Supporting Information). Dry CO_2 was fed to the sorbent first and then the CO_2 was desorbed at 75 °C. After the weight of the composite was back to the original weight at 30 °C, the CO_2 was bubbled through a water container before being fed into the TGA chamber for sorbent uptake at 30 °C. No enhancement of CO_2 uptake was observed.

In addition to the 100% CO_2 flow, we used a 10% CO_2 in alkane mixture (composed of 85% CH_4, 3% C_2H_6 and 2% C_3H_8) in order to mimic a natural gas field. The result still showed ~12 wt % maximum CO_2 uptake capacity for PEI-CMK-3 and ~13 wt % for PVA-CMK-3 (Figure 4a, b). When CH_4 was used as the pure gas feed, only 1.5 wt % CH_4 capacity was observed (Figure 4c). Hence, there is selectivity between CO_2 and CH_4 gas.

In conclusion, we have synthesized new and efficient CO_2 sorbents based on amine-modified mesocarbon CMK-3 composites through in situ polymerization. The synthesis process results in the entrapped polymers interpenetrating the composite frameworks of the mesocarbon CMK-3. A CO_2 sorption capacity of 13.4 wt % (3.52 mmol/g) was obtained, which is more than twice that of the pure CMK-3. The sorbents are readily and fully regenerated at a relatively low temperature, they exhibit stability over repetitive sorption-desorption cycles, and there is CO_2 selectivity over alkane gases.

MATERIALS AND METHODS

Mesoporous silica SBA-15 was used as a hard template to prepare mesocarbon CMK-3 as in the previous report.[16] In a typical preparation of SBA-15, $EO_{20}PO_{70}EO_{20}$ (Pluronic P123, 4.0 g) was dissolved in a solution of water (30 mL) and 2 M HCl (100 mL) with stirring at 35 °C. Tetraethylorthosilicate (TEOS, 8.50 g) was added into that solution with stirring at 35 °C for 20 h. The mixture was heated at 100 °C overnight without stirring. The solid product was recovered, washed, and vacuum dried at 100 °C. Calcination was carried out by slowly heating from room temperature in air to 500 °C over 8 h and then heating at 500 °C for 6 h.

The resulting mesoporous silica SBA-15 (0.50 g) was added to a solution of sucrose (0.625 g, 1.8 mmol, EMD Chemicals), H_2SO_4 (18 M, 0.04 mL, Fisher Scientific) and H_2O (5 mL, 277.8 mmol) in a 20 mL sample vial. After stirring 2 h at room temperature, the white slurry was dried in the vial at 100 °C for 6 h and then at 160 °C for another 6 h under air. The product was light brown, and was removed from the vial, ground with a mortar and pestle, then placed back in the vial. Second portions of sucrose (0.40 g, 1.2 mmol), water (5 mL, 277.8 mmol), and conc. H_2SO_4 (18 M, 0.03 mL) were added into the dried mixture, and the resulting dark brown slurry was stirred for 2 h at room temperature. The mixture was heated again in the same vial in an oven at 100 °C for 6 h and then 160 °C under air. The black product was removed from the vial and powdered using a mortar and pestle, then the powder was placed in a ceramic boat in a furnace and carbonized at 900 °C for 6 h under Ar. After cooling, the carbonized black powder was poured into a polypropylene bottle with 10% aqueous HF (400 mL) and the slurry was stirred for 6 h to remove the SiO_2. The slurry was filtered and the filter cake was washed with water until the filtrate was neutral by litmus paper. The filter cake was dried at 100 °C in a vacuum oven overnight to yield mesocarbon CMK-3 (0.50 g).

For the synthesis of the PEI-CMK-3 composite, CMK-3 (0.50 g) was suspended in a solution containing 2-methyl-2-oxazoline (1.5 g, 18 mmol) and acetonitrile (1.85 g, 45.1 mmol) in a 20 mL sample vial, and the black slurry was stirred for 6 h at room temperature. Then the acetonitrile was evaporated in a vacuum oven overnight at 80 °C, followed by adding a catalytic amount of $BF_3{\cdot}Et_2O$ (0.007 g, 0.05 mmol) to the product. The sealed vial was subsequently heated in an oven for 12 h at 90 °C for the polymerization step. The powder was transferred to a 250 mL round-bottom flask that contained 2 M aqueous NaOH (100 mL). The mixture was stirred and heated at 90 °C for 12 h. After cooling, the powder was recovered by filtration and the filter cake was washed with water until the filtrate was neutral to litmus paper. The product was dried in an oven at 100 °C overnight to yield ~0.70 g of PEI-CMK-3 composite. The PVA-CMK-3 composite was synthesized in a similar fashion: CMK-3 (0.50 g),

dx.doi.org/10.1021/am201278c | ACS Appl. Mater. Interfaces 2011, 3, 4782–4786

N-vinylformamide (0.30 g, 4.3 mmol) and 2,2′-azobis(2-methylpropionitrile) (AIBN, 0.03 g, 0.02 mmol) were mixed in THF (1.76 mL, 1.56 g, 21.7 mmol) and the mixture was stirred in a 20 mL sample vial for 6 h at room temperature. The vial was then heated in a 55 °C vacuum oven overnight. Additional portions of *N*-vinylformamide (0.30 g, 4.3 mmol) and 2,2′-azobis(2-methylpropionitrile) (AIBN, 0.03 g, 0.02 mmol) were added and the sealed vial was heated in a 90 °C oven for 12 h to produce a dark gray solid. The powder was transferred to a 250 mL round-bottom flask that contained 2 M aqueous NaOH (100 mL). The mixture was stirred and heated at 90 °C for 12 h. After cooling, the powder was recovered by filtration and the filter cake was washed with water until the filtrate was neutral to litmus paper. The product was dried in a vacuum oven at 80 °C overnight to yield 0.70 g of PVA-CMK-3.

■ ASSOCIATED CONTENT

Ⓢ Supporting Information

TGA plot and CO_2 uptake graph. This material is available free of charge via the Internet at http://pubs.acs.org.

■ AUTHOR INFORMATION

Corresponding Author

*E-mail: tour@rice.edu.

■ ACKNOWLEDGMENTS

This work was supported by the ONR MURI program (#00006766, N00014-09-1-1066) and the Advanced Energy Consortium (Baker Hughes, Halliburton, Conoco Phillips, bp, OXY, Marathon, Shell, Total, Petrobras, Schlumberger).

■ REFERENCES

(1) "International Space Station Environmental Control and Life Support System." NASA. http://www.nasa.gov/centers/ marshall/pdf/104840main_eciss.pdf.
(2) Puxty, G.; Rowland, R.; Allport, A.; Yang, Q.; Bown, M.; Burns, R.; Maeder, M.; Attalla, M. *Environ. Sci. Technol.* **2009**, *43*, 6427−6433.
(3) Siriwardane, R. V.; Shen, M. S.; Fisher, E. P.; Poston, J. A. *Energy Fuels* **2001**, *15*, 279−284.
(4) Heuchel, M.; Davies, G. M.; Buss, E.; Seaton, N. A. *Langmuir* **1999**, *15*, 8695−8705.
(5) Fryxell, G. E.; Liu, J.; Hauser, T. A.; Nie, Z.; Ferris, K. F.; Mattigod, S.; Gong, M.; Hallen, R. T. *Chem. Mater.* **1999**, *11*, 2148−2154.
(6) Yoshitake, H.; Yokoi, T.; Tatsumi, T. *Chem. Mater.* **2002**, *14*, 4603−4610.
(7) Xu, X.; Song, C.; Andresen, J. M.; Miller, B. G.; Scaroni, A. W. *Microporous Mesoporous Mater.* **2003**, *62*, 29−45.
(8) Caskey, S. R.; Wong-Foy, A. G.; Matzger, A. J. *J. Am. Chem. Soc.* **2008**, *130*, 10870−10871.
(9) McDonald, T. M.; D'Alessandro, D. M.; Krishna, R.; Long, J. R. *Chem. Sci.* **2011**, *2*, 2022−2028.
(10) Li, J.-R.; Ma, Y.-G.; McCarthy, M. C.; Sculley, J.; Yu, J.-M.; Jeong, H.-K.; Balbuena, P. B.; Zhou, H.-C. *Coord. Chem. Rev.* **2011**, *255*, 1791−1823.
(11) Bollini, P.; Didas, S. A.; Jones, C. W. *J. Mater. Chem.* **2011**, *21*, 15100−15120.
(12) Lee, J.; Han, S.; Hyeon, T. *J. Mater. Chem.* **2004**, *14*, 478−486.
(13) Ryoo, R.; Joo, S. H.; Kruk, M.; Jaroniec, M. *Adv. Mater.* **2001**, *13*, 677−681.
(14) Kyotani, T. *Carbon* **2000**, *38*, 269−286.
(15) Choi, M.; Ryoo, R. *Nature Mater.* **2003**, *2*, 473−476.
(16) Zhao, D.; Feng, J.; Huo, Q.; Melosh, N.; Fredrickson, G. H.; Chmelka, B. F.; Stucky, G. D. *Science* **1998**, *279*, 548−552.
(17) Joo, S. H.; Choi, S. J.; Oh, I; Kwak, J.; Liu, Z.; Terasaki, O.; Ryoo, R. *Nature* **2001**, *412*, 169−172.
(18) Mello, M. R.; Phanon, D.; Silverira, G. Q.; Llewellyn, P. L.; Ronconi, C. M. *Micropor. Mesopor. Mater.* **2011**, *143*, 174−179.
(19) Xu, X. C.; Song, C. S.; Andresen, J. M.; Miller, B. G.; Scaroni, A. W. *Energy Fuels* **2002**, *16*, 1463−1469.
(20) Choi, S.; Drese, J. H.; Jones, C. W. *ChemSusChem* **2009**, *2*, 796−854.
(21) Ma, X. L.; Wang, X. X.; Song, C. S. *J. Am. Chem. Soc.* **2009**, *131*, 5777−5783.
(22) Sayari, A.; Belmabkhout, Y. *J. Am. Chem. Soc.* **2010**, *132*, 6312−6314.